



ELSEVIER

Journal of Non-Crystalline Solids 191 (1995) 311–320

JOURNAL OF  
NON-CRYSTALLINE SOLIDS

# A study by density measurements and indentation tests of a calcium silicophosphate bioactive glass with different MgO or SrO contents

P.G. Galliano, A.L. Cavalieri, J.M. Porto López \*

*Instituto de Investigaciones en Ciencia y Tecnología de Materiales (INTEMA) –(CONICET–UNMdP), Av. J.B. Justo 4302,  
7600 Mar del Plata, Argentina*

Received 17 March 1993; revised manuscript received 10 May 1995

## Abstract

Vickers and Knoop indentation techniques and density measurements have been employed to study the structure of two series of glasses in the system  $\text{CaO-RO-SiO}_2\text{-P}_2\text{O}_5\text{-CaF}_2$  ( $\text{R} = \text{Sr, Ca, Mg}$ ) with: (a) constant alkaline earth oxide content, but using different cations ( $\text{Ca, Ca + Sr, Ca + Mg}$ ), and (b) increasing alkaline earth concentration ( $\text{Mg}$  and/or  $\text{Ca}$ ). Samples have been prepared by melting the raw materials at  $1400^\circ\text{C}$ , and pouring the liquid on a steel plate. From the experimental data, microhardness,  $H_V$ , fracture toughness,  $K_{IC}$ , and values for mean atomic volume,  $V_A$ , and ionic volume fraction,  $V_F$ , were obtained. The last parameter is proposed as a suitable one for the analysis of variations in cationic coordination numbers,  $n$ . The results show that  $\text{Mg, Ca}$  and  $\text{Sr}$  have similar values of  $n$ . The value of  $n$  is proposed to be six.

## 1. Introduction

Since the first studies by Hench et al. [1], several bioactive glass and glass-ceramic materials have been developed [2,3] and used as implants for bone replacement [2–4]. Among the most successful materials are the glasses of the system  $\text{CaO-MgO-SiO}_2\text{-P}_2\text{O}_5\text{-CaF}_2$ , from which Kokubo et al. [5] obtained the apatite-wollastonite glass-ceramic Cerabone<sup>TM</sup>. Although bioactivity of glasses depends on both their chemical composition and structure, to our knowledge few studies have dealt with the latter aspect.

Structural information about these glasses was obtained from Fourier transform infrared (FTIR), Raman and  $^{31}\text{P}$  and  $^{29}\text{Si}$  nuclear magnetic resonance (NMR) spectroscopic analyses [6]. The results showed that both P and Si are only present in four-coordinated sites. Phosphorus is located in  $(\text{PO}_4)^{3-}$  monomeric units, i.e., in an orthophosphate environment, surrounded by a silicate matrix composed of different Si-containing structural units having one, two and three non-bridging oxygens per  $\text{SiO}_4$  tetrahedra. These techniques provided information about Si and P covalent bonds and local environment, but they were not useful for the local order analysis of the alkaline-earth cations  $\text{Ca}^{2+}$ ,  $\text{Sr}^{2+}$  and  $\text{Mg}^{2+}$ , which represent at least half of the total amount of cations present in these glasses.

\* Corresponding author. Tel: +54-23 821 291. Telefax: +54-23 820 071.

As a consequence, other techniques need to be used to complement the spectroscopic data. Among them, density measurements have been widely used to study the effects of composition on glass structure. These measurements are usually employed to control the homogeneity of the glass, but the value of density itself is not a useful structural parameter. On the contrary, the determination of molar volume, mean atomic volume and oxygen molar volume from density data can provide information on different aspects of the glass structure, such as changes in coordination numbers,  $n$ , and degree of anionic packing and deformation [7–9].

Glass structure can also be studied by indentation methods [9,10]. As these measurements are performed on many different points of the surface, the obtained results (microhardness,  $H_V$ ; elastic modulus,  $E$ ; fracture toughness,  $K_{IC}$ ) are not strongly affected by local defects or heterogeneities. These properties are strongly dependent on several parameters [7–9], i.e., the degree of structural stiffness, coordination numbers, bond strength, elastic modulus and fracture energy,  $\gamma$ . For that reason, indentation methods can provide, from a physical standpoint, useful information about structural aspects of the glass.

All of these techniques have been widely employed in the analysis of soda-lime-like [7,11] and phosphate glasses [9,10] but, to our knowledge, very few results about alkaline earth silicate and silicophosphate glasses (i.e., alkali-free glasses) with high modifier cation contents have been reported. In this work, density, mean atomic volume,  $V_A$ , ionic

volume fraction,  $V_F$ ,  $H_V$  and  $K_{IC}$  values (the two last ones obtained from indentation methods) of two series of glasses in the system  $\text{CaO-RO-SiO}_2\text{-P}_2\text{O}_5\text{-CaF}_2$  ( $R = \text{Sr, Ca, Mg}$ ) have been obtained. The results have been interpreted in terms of structural aspects of the glasses, such as the cationic coordination number, and related to previous results obtained from spectroscopic techniques. All these samples showed the ability of developing a Ca- and P-rich surface layer after soaking them in simulated body fluid [12], a phenomenon which was reported to be directly correlated to *in vivo* bioactivity [3]. Although biocompatibility of a Sr-containing sample is unlikely, Sr (an element which has been widely used to trace the pathway of Ca in the body) was included in one of the samples in order to contribute, in a comparative way, to the study of the local structure of Ca and Mg (the two most widely employed alkaline earth cations in bioactive systems). The analysis of the local order of both cations is the main aim of this work.

## 2. Experimental

Two series of samples were prepared:

(A) with constant alkaline earth oxide content, but using different cations (Ca, Ca + Sr, Ca + Mg);

(B) with increasing alkaline earth concentration by additions of MgO to sample 1. The Si/P molar ratio (2.48) was maintained constant in all the samples.

Table 1  
Batch composition of the glasses used in this study (mol%)

Sample	CaO	MgO	SrO	SiO <sub>2</sub>	P <sub>2</sub> O <sub>5</sub>	RO	F/O ( $\times 10^{-3}$ )
<i>Series A</i>							
A0	47.01	7.15	–	38.15	7.69	54.16	5
1	54.16	–	–	38.15	7.69	54.16	5
A2	47.01	–	7.15	38.15	7.69	54.16	5
<i>Series B</i>							
1	54.16	–	–	38.15	7.69	54.16	5
B3	50.29	7.15	–	35.42	7.15	57.44	5
B4	46.79	13.61	–	32.96	6.64	60.40	5
B5	40.78	25.36	–	28.18	5.68	66.14	5

Raw materials ( $\text{MgO}$ ,  $\text{CaCO}_3$ ,  $\text{SrCO}_3$ , quartz,  $\text{H}_3\text{PO}_4$  and fluorite) were mixed in the desired proportions, melted at  $1400^\circ\text{C}$  for 240 min and quenched by pouring on a steel plate. The compositions of the glasses are given in Table 1.

The glass samples were annealed at  $650^\circ\text{C}$ , cut and polished with diamond paste ( $2.5\ \mu\text{m}$ ) and ethanol, in order to avoid chemical attack by water (FTIR specular reflectance spectra of the samples did not change after polishing). Then, the samples were again annealed (5 h at  $650^\circ\text{C}$ ) to relieve the stresses produced during polishing. The crystallization phenomenon was detected only at temperatures higher than  $730^\circ\text{C}$  [13].

The density of the samples was measured by the Archimedes method. Bulk samples were weighed at  $37^\circ\text{C}$  in air and also immersed in kerosene. From the density data, oxygen molar volume,  $V_O$ ,  $V_A$  and  $V_F$  of each sample were calculated. The experimental error of these data (Figs. 1–3) is indicated by the size of the symbols (in the case of  $H_V$  and  $K_{IC}$  data, the experimental error is represented by the length of the bar, as is shown in Figs. 4 and 5).

In order to obtain the values of  $H_V$  and  $K_{IC}$ , the polished surfaces were indented with loadings of 300 and 1000 g for 15 s using Vickers and Knoop indenters in a microhardness tester. At least 10 points were tested for each sample datapoint. Mean values of  $H_V$  were plotted, the experimental error being  $\leq \pm 0.25$  GPa. Crack patterns were observed around the Vickers indentations for both loadings.

$K_{IC}$  values obtained by the indentation fracture method were calculated from the average value of  $c$  using the equation proposed by Anstis et al. [14], with loadings of 1000 g:

$$K_{IC} = 0.016(E/H_V)^{1/2} P c^{-3/2}, \quad (1)$$

where  $P$  is the load,  $c$  is the crack length,  $E$  is Young's modulus and  $H_V$  is Vickers hardness.

The value of  $E/H_V$  was estimated from the measurement of the diagonals of the Knoop indentation, using the criterion proposed by Marshall et al. [15].

The results of series A are plotted against the mean cationic radius,  $r_{mc}$  (Figs. 1(a), 2(a), 3(a), 4(a) and 5(a)), calculated from ionic radius data [7]. The obtained values were 0.708, 0.727 and 0.741 Å for samples A0, 1 and A2 respectively.

### 3. Results

Figs. 1(a) and (b) show an increase in density with mean cationic radius (series A) and with RO content (series B). From these data, molar and mean atomic volumes could be obtained. Molar volumes are meaningless for this study, since the total number

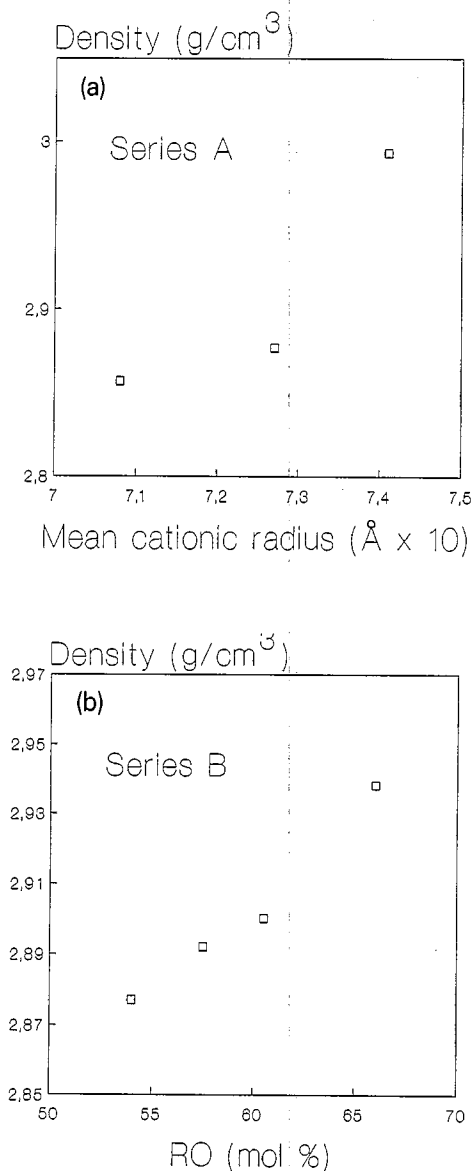


Fig. 1. (a) Density vs. mean cationic radius in series A. The error is indicated by the size of the data symbols. (b) Density vs. RO content (mol%) in series B. The error is indicated by the size of the data symbols.

of atoms per mole, in series B, is different in each sample. Then, only mean atomic volumes were obtained according to the formula

$$V_A = \sum_i x_i A_i / \delta, \quad (2)$$

where  $\delta$  is the measured density,  $x_i$  is the molar fraction of the atom  $i$  and  $A_i$  is the atomic weight.

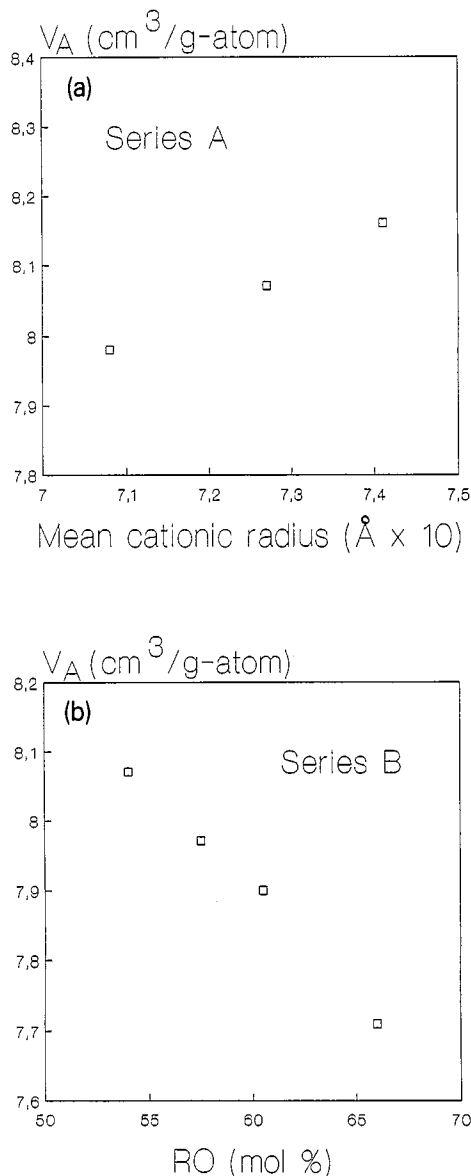


Fig. 2. (a) Mean atomic volume,  $V_A$ , vs. mean cationic radius in series A. The error is indicated by the size of the data symbols. (b) Mean atomic volume,  $V_A$ , vs. RO content (mol%) in series B. The error is indicated by the size of the data symbols.

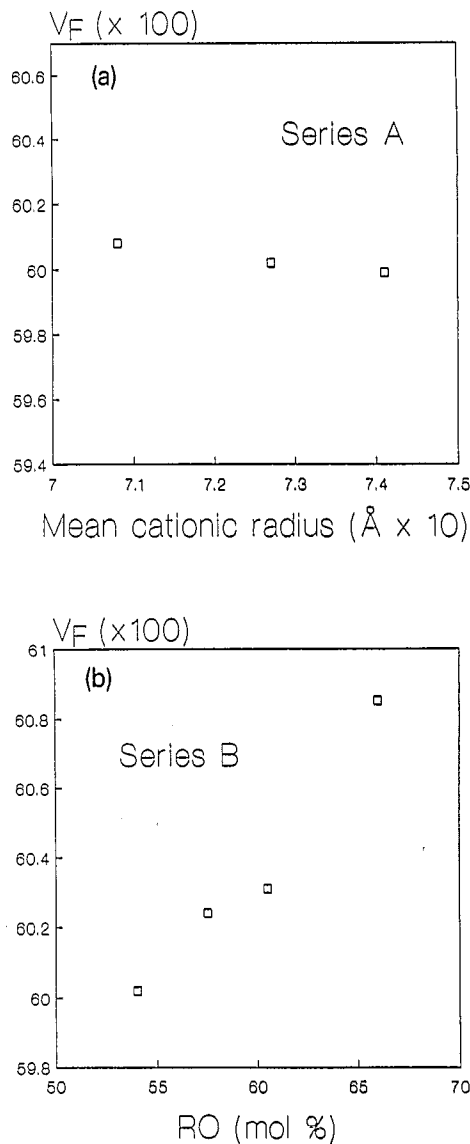


Fig. 3. (a) Ionic volume fraction,  $V_F$ , vs. mean cationic radius in series A. The error is indicated by the size of the data symbols. (b) Ionic volume fraction,  $V_F$ , vs. RO content (mol%) in series B. The error is indicated by the size of the data symbols.

Mean atomic volumes,  $V_A$ , are shown in Figs. 2(a) and (b). In series A,  $V_A$  increases with the mean cationic radius and, in the case of series B, a diminution of  $V_A$  with increasing RO content by MgO additions was observed. In this last series, the increase in RO content led to a decrease in the mean cationic radius.

Theoretical mean atomic volumes,  $V_T$ , have been calculated using

$$V_T = \sum_i (4/3) \pi r_i^3 x_i, \quad (3)$$

where  $r_i$  is the radius of the ion  $i$  and  $x_i$  is the molar fraction of the ion  $i$ .

The ratio of the theoretical and experimental atomic volumes was obtained for each sample. This ratio is called ionic volume fraction,  $V_F$ , and pro-

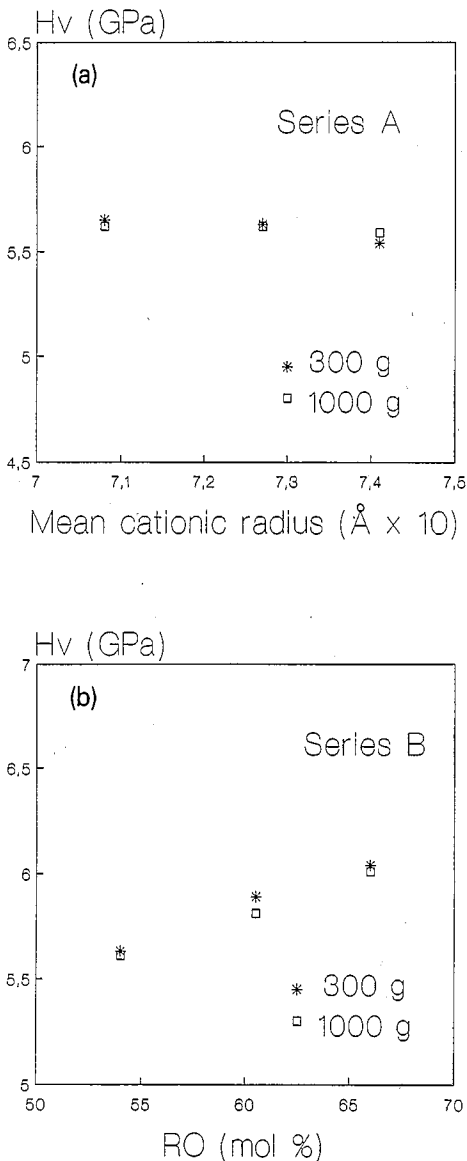


Fig. 4. (a) Vickers hardness number,  $H_v$ , vs. mean cationic radius in series A. (b) Vickers hardness number,  $H_v$ , vs. RO content (mol%) in series B.

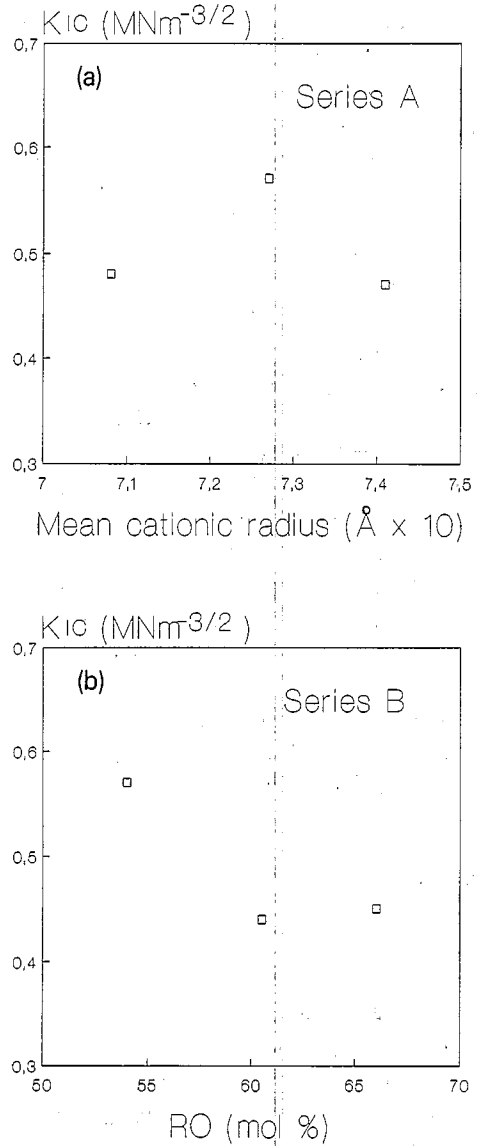


Fig. 5. (a) Fracture toughness,  $K_{IC}$ , vs. mean cationic radius in series A. (b) Fracture toughness,  $K_{IC}$ , vs. RO content (mol%) in series B.

vides an estimation of the degree of packing of the ions in the glass ( $V_F$  is also defined in the literature as the ratio between the theoretical and experimental molar volumes) [16]. We must point out that theoretical mean atomic volumes are calculated from simple geometrical considerations by using ionic radii data, and do not take into account any structural variation (i.e., coordination number change) which can affect the density of the glass.

The results of  $V_F$  are plotted in Figs. 3(a) and (b), and show no changes in this value within series A. By contrast, an increase in  $V_F$  with increasing RO can be observed in series B.

Fig. 4(a) shows the Vickers hardness numbers,  $H_V$ , of the samples of series A. No changes have been observed in this series. On the other hand, microhardness of the samples in series B (Fig. 4(b)) increases at higher alkaline earth contents, from 5.63 GPa for sample 1 to 5.89 GPa for sample B4 and 6.04 GPa for sample B5.

Results obtained from the Knoop indentation measurements by using the criterion proposed by Marshall et al. [15] showed that the values of  $E$  in series B increase about 7% from sample 1 to B5, and show no variation in series A. These data were employed in the calculation of  $K_{IC}$ .

In Figs. 5(a) and (b), the  $K_{IC}$  values obtained from Eq. 1 are plotted. Fig. 5(a) shows that  $K_{IC}$  values of samples A2 and B0 are about 24% lower than that of sample 1. In series B, the difference between the results from samples B4 and B5 was negligible, but both of them have  $K_{IC}$  values significantly lower (22%) than that of sample 1 (Fig. 5(b)).

## 4. Discussion

### 4.1. Density

In series A, both density (Fig. 1(a)) and mean atomic volume (Fig. 2(a)) increase with mean cationic radius. This means that the increase in density is due to the greater atomic weight of Sr with respect to Ca and Mg, in spite of the increase in  $V_A$ , when going from Mg (sample B0) to Sr (sample B2). By contrast, in series B, both the decrease in  $V_A$  and the increase in the mean atomic weight of the system from sample 1 to B5 contribute to the observed increase in density (Fig. 1(b)).

### 4.2. Local order of Ca, Mg and Sr in alkaline-earth silicates and phosphates

Recent results obtained by extended X-ray absorption fine structure, neutron scattering and X-ray diffraction [17,18] showed a coordination number of six for Ca in

(a) a series of alkaline-earth silicate glasses, with similar RO contents to those of the glasses studied in this work, and

(b) polycrystalline wollastonite ( $\text{CaSiO}_3$ ), which is one of the phases which results from the crystallization of these glasses.

To our knowledge, there are no data about the local environment of Sr and Mg in alkaline-earth silicophosphate glasses and related systems. However, it is important to mention that Ca and Sr usually present a complete solid solubility range in crystalline alkaline-earth silicates [19] and phosphates [20]. This, together with the similitude in their ionic radii, strongly suggest that the coordination number of Ca,  $n_{Ca}$ , and Sr,  $n_{Sr}$ , in these glasses must be the same.

In the case of alkaline-earth phosphates, Ca, Sr and Mg have been reported to be present in six-coordinated sites, while Mg has been also reported to be fourfold-coordinated. Ca and Sr also present octahedral polyhedra around them in the structure of apatite [21], a crystalline phase which was also obtained from the devitrification of the glasses studied in this work [13].

Taking all these reasons into account, we can expect in our system one of the following possible situations:

(a)  $n_{Ca} = n_{Sr} > n_{Mg}$  (6, 6 and 4, respectively, is the most likely configuration. However the system might also present Ca and Sr in cubic sites,  $n = 8$ , and six-coordinated Mg);

(b)  $n_{Ca} = n_{Sr} = n_{Mg}$  (in this case,  $n$  must be 6). Both possibilities are discussed in Sections 4.3.–4.5.

### 4.3. Mean atomic volume

Molar and mean atomic volume,  $V_A$ , of glasses have been reported to decrease with the coordination numbers of the components of the system [7–10], and to increase with their ionic radii [7–11].

Fig. 2(a) shows that  $V_A$  increases almost linearly with the cationic radius (series A), being the Mg-containing sample (sample A0) which has the smallest volume. Higher values of  $V_A$  are expected for the samples containing low-coordination number cations (low-coordination cations lead to less dense packing than high-coordinated cations). At this point, it is important to take into account that this result can be

in agreement with any of the possible Mg coordination numbers: even if  $n_{\text{Mg}}$  were lower than  $n_{\text{Ca}}$ , the percentage of replaced Ca (13%) is probably low enough to justify an increase in the absolute value of  $V_{\text{A}}$ .

In series B, the addition of Mg results in a diminution of the total content of Ca, P and Si, the last two being four-coordinated cations (see Table 1). In this case, a diminution of  $V_{\text{A}}$  with increasing MgO and RO content was observed (Fig. 2(b)). However, the mean cationic radius increases from sample 1 to B5. The observed result can be explained if the mean cationic coordination number (the average of the coordination numbers of all the cations in the system) is increasing from sample 1 to B5, although the mean cationic radius is also increasing (0.0727 nm in sample 1, and 0.0742 nm in sample B5). An increase in  $V_{\text{A}}$  with  $r_{\text{mc}}$  can be explained if the mean cationic coordination number,  $n_{\text{mc}}$ , is also increasing in the same direction. An increase in  $n_{\text{mc}}$  can be only expected if  $n_{\text{Mg}}$  is

- (a) higher than  $n_{\text{P}}$  and  $n_{\text{Si}}$  ( $n_{\text{Mg}} > 4$ ), and
- (b) not lower than  $n_{\text{Ca}}$ , which is in agreement with the idea of a coordination number of 6 for both Ca and Mg.

#### 4.4. Ionic volume fraction

The values of  $V_{\text{A}}$  which are already discussed are affected by both the ionic radii of the cations and their coordination numbers. In order to analyze the local environment of the cations of these glasses, another structural parameter is proposed to be studied: the ionic volume fraction,  $V_{\text{F}}$ . This parameter results from the ratio between the experimental and theoretical values of the mean atomic volume, and can be considered a measure of the packing degree of the glass structure [16] or of  $n_{\text{mc}}$ .

The calculated theoretical values of mean atomic volumes,  $V_{\text{T}}$ , are smaller than the experimental ones, which were obtained from density measurements (about 60% of these values). This is due to the quite poor ionic packing condition of these glasses. For example, it was observed [12] that the density of sample B3 after being partially crystallized into an apatite-wollastonite glass ceramic is 5% higher than that of its parent glass.

The results of  $V_{\text{F}}$  (Figs. 3(a) and (b)) show some interesting features. In series A, the strong similitude

between the values of  $V_{\text{F}}$  (Fig. 3(a)) indicates that there is no difference between the coordination numbers of the alkaline earth cations. A low-coordinated Mg would result in a less packed structure in sample A0, a phenomenon which does not agree with the results of  $V_{\text{F}}$ .

Fig. 3(b) shows an increment in  $V_{\text{F}}$  from sample 1 to B5 (series B). This behavior can be only understood if we assume that the additions of six-coordinated Mg result in an increment in the  $n_{\text{mc}}$  of the system (in this series, addition of Mg results in a diminution of the total content of Ca, P and Si, the last two ones being four-coordinated cations). Again in this case, this result is not expected if the coordination number of Mg was 4, since in this case  $n_{\text{mc}}$  would decrease along the series. The observed increment in  $V_{\text{F}}$  cannot be explained either if the coordination number of Ca, Sr and Mg were 8, 8 and 6, respectively, because in this case  $n_{\text{mc}}$  remains unchanged.

#### 4.5. Microhardness and fracture toughness

Microhardness is related to quite complicated behaviors of resistance to superficial mechanical strains [9], which are, in the case of glasses, strongly influenced by viscosity. For silicate glasses with high Si content, in which both microhardness and viscosity depend on the alkaline and alkaline earth cation concentration [22], it was found that viscosity at low temperatures is not affected by the amount of broken silicon-oxygen bonds, but strongly depends on the coordination number of cations [23]. For that reason, an important contribution of the cationic coordination number to the values of microhardness is expected.

One important contribution to the study of microhardness in glasses was made by Yamane and Mackenzie [16], who related  $H_{\text{V}}$  to different structural parameters:

$$H_{\text{V}} = 0.051 \left( \alpha / [0.462 + 0.09V_{\text{F}} - V_{\text{F}}^2] \right)^{1/2} E, \quad (4)$$

where  $\alpha = \sum \{f_i n_i \epsilon_i\} / (\epsilon_{\text{Si}} \sum \{f_i n_i\})$  is the average single bond strength,  $f$  is the number of cations  $i$  in 1 mol of glass,  $n$  is the coordination number,  $V_{\text{F}}$  is the ionic volume fraction (see above, Section 4.4.,  $E$  is Young's modulus,  $\epsilon$  is the single bond strength of

cation  $i$  to oxygen bond and  $\epsilon_{\text{Si}}$  is the single bond strength of the Si–O bond.

Finally, it is important to mention that anomalous low  $H_V$  values were reported for  $\text{MgO} \cdot \text{P}_2\text{O}_5$  glasses with four-coordinated Mg, with respect to glasses with six-coordinated Ca, Sr, Ba and even Mg [9].

Fig. 4(a) shows the Vickers hardness numbers,  $H_V$ , of the samples of series A. No changes have been observed in this series, showing that the nature of the alkaline earth cation, in this concentration range, does not affect microhardness. If the results were interpreted in terms of cationic coordination number, as we did in the case of the mean atomic volume data, they would show that this number must be the same for the alkaline earth cations in all the samples of the series.  $H_V$  did not change because of the constant value of the mean cationic coordination number, since Mg and Sr are assumed to substitute only for Ca, without modifying its coordination number.

A similar conclusion is obtained when microhardness results are interpreted in terms of the variation of the parameters in Eq. 4. It is important to remark that the equation was obtained for glasses with  $V_F < 0.55$ , and the values of  $V_F$  in our glasses are higher than 0.59. This is probably the main reason why, although the predicted results show a trend along the series similar to the experimental ones, the absolute values are not the same. Anyway, a non-quantitative analysis of the effect of compositional changes on the equation parameters can be done. For that purpose, we must take into account that Eq. (4) shows that  $H_V$  increases with four important parameters:  $\epsilon$ ,  $E$ ,  $V_F$  and  $n$ . It is of interest to point out the relative importance of  $n$ , since  $E$  and  $V_F$  strongly depend on it.

An estimation of the values of  $E$  was obtained by using the criterion proposed by Marshall et al. [15]. The  $H_V/E$  ratio was found to be 0.068 for all the samples. From this ratio,  $E$  values of all the samples were calculated using the  $H_V$  values previously obtained, and showed: (a) no variations along series A (the value of  $E$  for these samples was estimated to be 83.6 GPa), and (b) a total increment of 7% from sample 1 to B5 (series B). Although the error of the method proposed by Marshall et al. lies between 5 and 10%, the values obtained are in good agreement with data previously obtained by using a cubic resonance method [24].

Then, taking into account the constant value of  $E$  along series A and the observed decrease on  $V_F$  from sample A0 to sample A2 (series A, Fig. 3(a)), the constant value of  $H_V$  (Fig. 4(a)) can only be explained if there is a small increase in  $\alpha$  from sample A0 to sample A2 ( $\alpha$  was calculated from single bond strength data obtained from Refs. [25,26]). This increment is only possible if the values of  $n_i$  are the same along the series (i.e.,  $n_{\text{Mg}} = 6$ ), as was concluded in (b). By contrast, if  $n_{\text{Mg}}$  were lower than  $n_{\text{Ca}}$  and  $n_{\text{Sr}}$ , we should expect for this series a decrease in  $\alpha$  from sample A0 to A2, while the observed  $V_F$  decreased. Both phenomena would result in lower  $H_V$  values, which are not observed.

On the other hand, microhardness of the samples in series B (Fig. 4(b)) increases at higher alkaline earth contents, from 5.63 GPa for sample 1 to 5.89 GPa for sample B4 and 6.04 GPa for sample B5. In this series, Mg addition results in a diminution of the total content of Ca, P and Si (the last two being four-coordinated cations). A simple interpretation of these results based on the increment of the mean cationic coordination number along the series is not possible in this case, as we shall see below.

Results obtained from the Knoop indentation measurements showed that the values of  $E$  in series B increase about 7% from sample 1 to B5. The average bond strength of the system decreases from sample 1 to B5, leading to an increment in  $\alpha$  and  $H_V$ , regardless of the coordination number of Mg. By contrast, the increment of  $V_F$  along the series (Fig. 3(b)) produces an opposite effect on  $H_V$ . Eq. (4) indicates that, in this case, the increment of  $E$  should be the most important contribution to the observed increment in  $H_V$  along the series.

In Figs. 5(a) and (b), the  $K_{\text{IC}}$  values obtained from Eq. (1) are plotted. Fig. 5(a) shows that  $K_{\text{IC}}$  values of samples A2 and B0 are about 24% lower than that of sample 1. In series B, the difference between the results from samples B4 and B5 was negligible, but both of them have  $K_{\text{IC}}$  values significantly lower (22%) than that of sample 1 (Fig. 5(b)). At this point, it is important to say that the values of another important structural parameter, the glass transition temperature,  $T_g$ , showed the same trend in both series as these values of  $K_{\text{IC}}$ , suggesting that both behaviors are related to the bulk structure of the glass [13].

Fracture toughness of glasses depends on elastic



modulus,  $E$ , and fracture energy,  $\gamma$ . It is clear that the latter term plays an important role, since  $E$  is unchanged in series A while  $K_{IC}$  shows differences between the samples of this series. Fracture energy of glasses includes plastic deformation, surface energy and crack branching as its principal contributors. According to the low  $K_{IC}$  values, high Young's modulus and high ionic character of these glasses, it is reasonable to neglect the importance of plastic deformation mechanisms.

For an evaluation of the eventual role of the other factors affecting  $\gamma$  and, as a consequence,  $K_{IC}$ , a deeper understanding of the glass structure of this system is needed. However, it must be taken into account that Raman and  $^{31}\text{P}$  and  $^{29}\text{Si}$  NMR spectroscopic analyses of the samples of series A showed no differences in the number of non-bridging oxygens and in the local structure of Si and P [6]. This means that the relative amount of non-bridging oxygens and the relative distribution of  $Q^n$  species cannot justify, as a unique parameter, the trend in the  $K_{IC}$  values, as was previously reported [27]. Further analyses on this topic are now under study.

## 5. Conclusions

(1) The mean atomic volume,  $V_A$ , of the samples increases with the mean cationic radius,  $r_{mc}$ , in series A, while microhardness,  $H_V$ , and ionic volume fraction,  $V_F$ , are not affected. These trends are attributed to an invariance in the coordination number of R (R = Ca, Sr, Mg).

(2) In series B,  $V_A$  decreases with RO content, while  $H_V$  and  $V_F$  increase. These effects are explained through an increment in the mean cationic coordination number, due to the fact that Ca and Mg present the same coordination number, which is higher than that of P and Si.

(3) According to previous results in related systems, the value of the coordination number of Ca, Mg and Sr in these glasses is proposed to be 6.

(4) The values of  $V_A$  increase with the  $r_{mc}$  of the system in series A, and decrease with  $r_{mc}$  in series B. This is due to the fact that  $V_A$  is affected by both the ionic radii and the coordination numbers,  $n$ , of the cations. By contrast,  $V_F$  is mainly affected by  $n$ .

(5) The microhardness behavior can be qualitatively interpreted in terms of Yamane's equation [16], and the results agree with the proposed values of  $n$ . The increment of microhardness along series B is mainly attributed to an increment in the value of Young's modulus,  $E$ , estimated from Knoop indentation measurements.

(6) The increase in RO content (series B) and the presence of a second alkaline-earth oxide in the system (series A) resulted in a decrease in the  $K_{IC}$  values. The same trend was observed in both series for the values of the glass transition temperature,  $T_g$ .

(7) The relative amount of non-bridging oxygens and the relative distribution of  $Q^n$  species cannot explain, as an only parameter, the trend in the  $K_{IC}$  values.

The authors want to acknowledge the helpful comments and suggestions of Professor Naohiro Soga (Kyoto University) and Dr Eduardo Mari (IN-TEMIN).

## References

- [1] L.L. Hench, R.J. Splinter, W.C. Allen and T.K. Greenlee, J. Biomed. Mater. Symp. no.2 (part 1) (1972) 117.
- [2] L.L. Hench, J. Am. Ceram. Soc. 74 (1991) 1487.
- [3] T. Kokubo, in: Third Euro-Ceramics, ed. P. Durán and J.F. Fernández, Vol. 3 (Faenza, 1993) p. 1.
- [4] T. Yamamuro, J. Shikata, H. Okumura, T. Kitsugui, Y. Kakutani, T. Matsui and T. Kokubo, J. Bone Joint Surg. 72b (1990) 889.
- [5] T. Kokubo, S. Ito, S. Sakka and T. Yamamuro, J. Mater. Sci. 21 (1986) 536.
- [6] P.G. Galliano, J.M. Porto López, E. Varetto, I. Sobrados and J. Sanz, Mater. Res. Bull. 29 (1994) 1297.
- [7] J.M. Fernández Navarro, in: El Vidrio: Constitución, Fabricación, Propiedades, CSIC-ICV, Madrid, 1985, p. 97.
- [8] N. Soga, J. Non-Cryst. Solids 73 (1985) 305.
- [9] K. Hirao, M. Yoshimoto, N. Soga and K. Tanaka, J. Non-Cryst. Solids 130 (1991) 784.
- [10] N. Soga, Y. Sagawa, M. Yoshimoto and K. Hirao, Nippon Kagaku Kaishi no. 6 (1988) 886.
- [11] L. Shartsis, S. Spinners and W. Capps, J. Am. Ceram. Soc. 35 (1952) 155.
- [12] P.G. Galliano, PhD thesis, Universidad de Mar del Plata, (1994) p. 157–189.
- [13] P.G. Galliano and J.M. Porto López, J. Mater. Sci: Mater. Med., in press.

- [14] G.R. Anstis, P. Chantikul, B. Lawn and D.B. Marshall, *J. Am. Ceram. Soc.* 64 (1981) 533.
- [15] D.B. Marshall, T. Noma and A.G. Evans, *J. Am. Ceram. Soc.* 65 (1982) C-175.
- [16] M. Yamane and J.D. Mackenzie, *J. Non-Cryst. Solids* 15 (1974) 153.
- [17] M.C. Eckersley, P.H. Gaskell, A.C. Barnes and P. Chieux, *Nature* 335 (1988) 525.
- [18] J.M. Combes, in: *Proc. 16th Int. Congr. on Glass*, *Bol. Soc. Esp. Ceram. Vid.* 31-C (1992) 3.
- [19] P. Eskola, in: *Phase Diagrams for Ceramists* (American Ceramic Society, Westerville, OH, 1965) fig. 620.
- [20] J.F. Sarver, F.A. Hummel and M.V. Hoffman, in: *Phase Diagrams for Ceramists* (American Ceramic Society, Westerville, OH, 1965) fig. 623.
- [21] H. Aoki, *Medical Applications of Hydroxyapatite* (Ishiyaku Euroamerica, Tokyo, 1994) p. 227.
- [22] E.A. Mari, *Los Vidrios* (América, 1982) p. 99.
- [23] A.G.F. Dingall and H. Moore, *J. Soc. Glass Technol.* 37 (1953) 316.
- [24] T. Goto and N. Soga, *Yogyo-Kyokai-Shi* 91 (1983) 24.
- [25] R.C. Weast, ed., *CRC Handbook of Chemistry and Physics*, 56th Ed. (CRC, Boca Raton, FL) p. 216.
- [26] K. Sun, *J. Am. Ceram. Soc.* 30 (1947) 277.
- [27] A.S. Rizkalla, D.W. Jones and E.J. Sutow, *Br. Ceram. Trans. J.* 91 (1992) 12.